



# Manassantin A and B are Potential Therapeutic Agents for Treating Nonalcoholic Fatty Liver Disease

John Min<sup>1</sup>, Sin-Hee Han<sup>2</sup>, Ae-Jin Choi<sup>2</sup>, Faridoddin Mirshahi<sup>1</sup>, Shunlin Ren<sup>1</sup>, Jason D. Kang<sup>3</sup>, Phillip B. Hylemon<sup>3</sup>, Hae-Ki Min<sup>1\*</sup>, Arun J. Sanyal<sup>1\*</sup>

<sup>1</sup>Department of Internal Medicine, Division of Gastroenterology, Hepatology and Nutrition, Virginia Commonwealth University School of Medicine, Richmond, VA, USA; <sup>2</sup>Department of Herbal Corp Research, NIHHS, RDA, 92 Bisanro, EuMseong, Chungbuk, 369-873, Republic of Korea; <sup>3</sup>Department of Microbiology and Immunology, Virginia Commonwealth University, Richmond, VA, USA

## ABSTRACT

Manassantin (MNS) has been reported to have various biological activities including repression of Hypoxia-Inducible Factor 1 (HIF-1), anti-inflammatory, and anti-plasmodial properties. Here, we investigated whether MNS has the potential to serve as a therapeutic agent for treating Non-Alcoholic Fatty Liver Disease (NAFLD) *via* regulation of hepatic AMPK and ERK1/2, gp130/Stat3, inflammation, and autophagy pathways. In NAFLD patients, AMPK $\alpha$  (Thr172) phosphorylation levels were suppressed, whereas ERK1/2 phosphorylation levels were increased. In addition, IL-6 levels were directly correlated with ERK1/2 activation and were inversely related to decreases in AMPK $\alpha$  (Thr172) phosphorylation. MNS increased activation of AMPK $\alpha$  by increasing cellular AMP: ATP ratio, decreased ERK1/2 and PKC- $\theta$  phosphorylation, and decreased p62 and LC3 protein expression in palmitate (PA) or IL-6-treated human hepatocytes. PA or IL-6-induced-Stat3 phosphorylation levels were markedly suppressed in MNS-A or MNS-B treated-hepatocytes. There were no changes in histology and body weight in normal mice that were treated with MNS-B for 2 weeks. However, MNS-B upregulated hepatic AMPK phosphorylation and inhibited ERK phosphorylation in these mice showing that the compound may cause an energy deficient state in the normal animal model. This energy-deficient state may prove to be key in ameliorating diet-induced NAFLD. These results strongly suggest that MNS-A and MNS-B, plant-based compounds, modulate nutrient and inflammatory signaling pathways involved in NAFLD and appear to be promising therapeutic agents for treating NAFLD.

**Keywords:** Nonalcoholic steatohepatitis; Liver; Hepatocyte; AMPK; Steatosis; Manassantin

## INTRODUCTION

Nonalcoholic Fatty Liver Disease (NAFLD) is the most common cause of chronic liver disease and affects about 30 percent of the adult population in the US [1,2]. NAFLD is associated with many physiological factors including insulin resistance, autophagy, apoptosis, inflammation, and metabolic syndrome (obesity, lipotoxicity, combined hyperlipidemia, and diabetes mellitus (type II)) [3,4]. NASH is an aggressive form of NAFLD that affects 3-4 percent of NAFLD patients and can progress to cirrhosis in 15-20% of affected individuals [2,5]. Although the pathogenesis of NAFLD (progression from steatosis to NASH) is not yet fully understood, much progress has been made in recent years in elucidating the mechanisms of the progression from NAFLD to NASH [6-8].

The prevention and treatment of NAFLD have been extensively studied but there are no approved standard medical treatments other than changes in diet and exercise. In the early stages, a

healthy diet and regular exercise may help to prevent NAFLD [9]. This includes weight loss, the prevention of type II diabetes, and lowering of serum cholesterol and triglycerides. Some drugs including plant-based compounds appear to improve serum markers for liver injury but do not improve hepatic histology in NAFLD [10-12].

MNS-B, from *Saururus Chinensis*, has been reported to inhibit the production of IL-1 $\beta$  and attenuate the phosphorylation of ERK1/2 and p38 MAPK, but not that of JNK, in LPS-treated RAW 264.7 cells [13]. Moreover, MNS-A and B have been reported to have various positive biological activities such as anti-inflammatory [13] and anti-plasmodial properties [14]. The use of natural products for the treatment of NAFLD has not been explored in depth. Even though several studies have reported that natural plant compounds play an important role in the treatment of various human diseases, the mechanisms underlying how they affect NAFLD remain unclear.

**Correspondence to:** Hae-Ki Min, Department of Internal Medicine, Division of Gastroenterology, Hepatology and Nutrition, Virginia Commonwealth University School of Medicine, Richmond, VA, USA, Tel: 804 828 6314; Fax: 804 828 5348; hae-ki.min@vcuhealth.org

Arun J Sanyal, Department of Internal Medicine, Division of Gastroenterology, Hepatology and Nutrition, Virginia Commonwealth University School of Medicine, Richmond, VA, USA, Tel: 804 828 6314; Fax: 804 828 5348; E-mail: arun.sanyal@vcuhealth.org

**Received:** 24-Feb-2022, Manuscript No. BOM-22-15695; **Editor Assigned:** 26-Feb-2022, Pre QC No. BOM-22-15695(PQ); **Reviewed:** 10-Mar-2022, QC No 15695; **Revised:** 10-Mar-2022, Manuscript No. 15695(R); **Published:** 16-Mar-2022, DOI: 10.35248/2167-7956.22.11.196.

**Citation:** Min J, Han S H, Choli A J, Mirshahi F, Ren S, Kang JD, et al. (2022) Manassantin A and B are Potential Therapeutic Agents for Treating Nonalcoholic Fatty Liver Disease. *J Biomol Res Ther.* 11:196.

**Copyright:** © 2022 Min J, et al. This is an open-access article distributed under the terms of the Creative Commons Attribution License, which permits unrestricted use, distribution, and reproduction in any medium, provided the original author and source are credited.

The overall goal of this study was to define the cross-talk between AMPK and ERK1/2 signaling pathways, which are considered to be relevant for NAFLD-related hepatic inflammation and lipid accumulation. Here, we show that AMPK $\alpha$  phosphorylation levels were comparable in both control patient groups but were significantly lower in those with either NAFLD or NASH. In contrast, ERK1/2 phosphorylation levels were significantly increased in the NAFLD and NASH patient groups. Based on the role of these dysregulated cell signaling pathways in the pathophysiology of NAFLD, we examined the effects of MNS-A and B in treating NAFLD *in vitro*. In this regard, MNS-A and B

inhibited ERK1/2 phosphorylation and activated AMPK $\alpha$  levels, which led to a decrease in inflammation, lipid accumulation and induce autophagy in palmitate or IL-6-treated hepatocytes. Gp130-stat3 axis was directly suppressed by MNS-A and MNS-B in IL-6 and/or palmitate-induced hepatocytes. The histological progression and molecular signature on MNS-B treated-mice were not changed while hepatic AMPK phosphorylation was increased and ERK phosphorylation was inhibited. Based on the results of our studies, we propose that MNS may be useful as a therapeutic agent for the prevention and treatment of NAFLD.

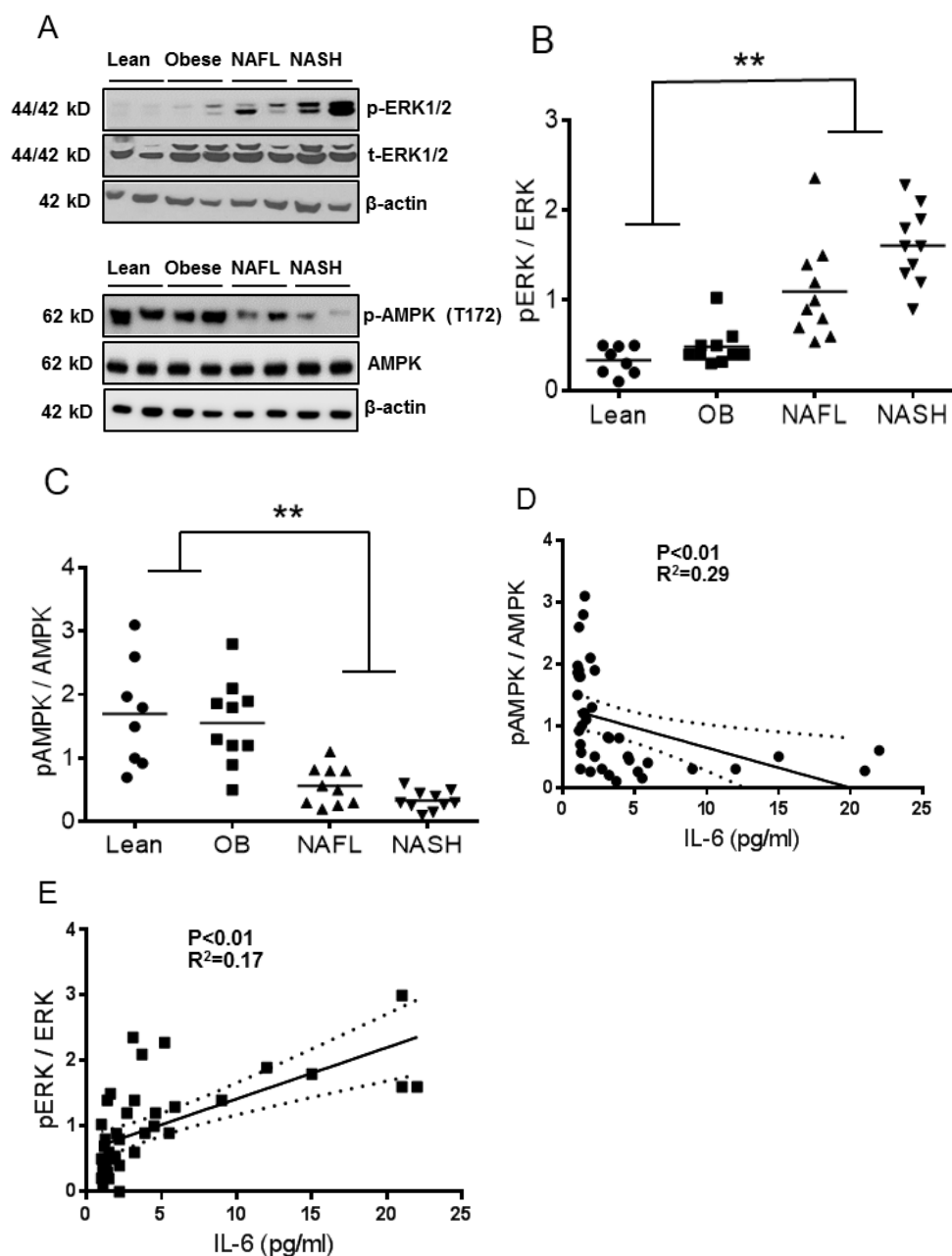


**Figure 1:** Human hepatic ERK1/2 and AMPK phosphorylation levels, and serum IL-6 levels. A-C Hepatic ERK1/2 and AMPK phosphorylation levels were examined in subjects with Non Alcoholic Fatty Liver (NAFL), Non Alcoholic Steato Hepatitis (NASH) (n=10 each), compared to lean (n=8) and weight-matched controls (n=10) with normal liver histology. Hepatic ERK1/2 phosphorylation progressively increased while AMPK phosphorylation levels decreased from lean normal to obese controls to NAFL and then to NASH (panel A-C, controls *vs.* NAFL or NASH  $p<0.01$ ). D-E. Circulating IL-6 protein was increased in both NAFL and NASH compared to lean and obese controls. Circulating IL-6 was inversely related to AMPK phosphorylation (panel D) while ERK1/2 was directly related to serum IL-6 levels (panel E). Individual data points or mean  $\pm$  S.D. are shown.

## MATERIALS AND METHODS

### Reagents

Primary antibodies including rabbit anti-pAMPK, rabbit anti-pERK, rabbit anti-tERK, rabbit anti-PARP, U0126, AICAR, IL-6 and ERK inhibitor PD 184352 were purchased from Cell Signaling (Beverly, MA, USA). The rabbit anti-gp130 primary antibody was purchased from Santa Cruz Biotechnology (Dallas, TX, USA). RIPA buffer, protease inhibitor mixture, ammonium chloride, leupeptin, cryovials, and Free Fatty Acid (FFA) were purchased from Sigma-Aldrich (St. Louis, MO, USA). HRP-conjugated secondary antibody and SuperSignal chemiluminescence kits were purchased from Pierce Biotechnology Inc. (Rockford, IL, USA). Cell culture media, Bovine Serum Albumin (BSA), and western blot supplies were purchased from Invitrogen (Carlsbad, CA, USA). Purified MNS-A and B from *Saururus Chinensis* were obtained from the Rural Development Administration (RDA) of the Republic of Korea.

### Human subjects

Four groups of subjects were enrolled in this study: 1) subjects with histologically-proven NASH, 2) subjects with histologically proven nonalcoholic fatty liver (NAFL), and subjects with normal liver histology who were either lean or obese. Lean normal (BMI<25) and obese (BMI>30) controls were defined by normal liver histology, liver enzymes, and function. Liver histology was evaluated by a single experienced liver pathologist. A fatty liver was defined by the presence of greater than 5% steatosis. Steatohepatitis and the nonalcoholic nature of the disease were defined in previous studies [6,7]. Concurrent subjects with the metabolic syndrome and suspected NAFLD were considered for this study prior to a clinically indicated liver biopsy. NAFLD was suspected from one or more of the following: hepatomegaly, elevated liver enzymes, and abnormal hepatic imaging. Liver tissue and biopsy for control groups were also obtained from an anonymous tissue repository at the investigators institution [7]. The liver biopsies were snap frozen in liquid nitrogen and stored at -80°C for analysis. All subjects provided informed consent and the study was approved by the institutional IRB (VCU IRB # 1960). Blood samples were obtained from each patient at the time of liver biopsy, processed to serum, and stored at 80°C.

### Serum sample collection and ELISA assay

Serum sample collection and ELISA assay were performed as previously described [15]. Briefly, serum patients underwent a peripheral venipuncture collection of a 10-mL blood sample in red-topped tubes. The blood sample was centrifuged and the serum fraction was isolated. Serum samples were frozen at -80°C for an Enzyme-Linked Immunosorbent Assay (ELISA) analysis. The serum was subsequently used for quantitative measurement of IL-6 by a commercially available Enzyme-Linked Immunosorbent Assay (ELISA) kit (R and D Systems, Minneapolis, MN). All assays were performed in triplicate, and the absorbance was determined using a microplate reader (Infinite F50, Sn Jose, CA, USA).

### Cell cultures and palmitate treatments

Human primary hepatocytes ( $5-8 \times 10^6$  cells/ml) were obtained from Invitrogen (Carlsbad, CA, USA) and were cultured according to the supplier's protocols. Human Huh-7 cell line was grown in DMEM (Dulbecco Modified Eagle Medium) containing 10% Fetal Bovine Serum (FBS), 100 IU/ml penicillin, and 100 µg/ml

of streptomycin in a CO<sub>2</sub> incubator at 37°C. Purified MNS-A and B compounds were dissolved with methanol and added to cells prior to palmitate or reagent treatments. The palmitate treatment to cell exposure was performed as a previous described [6-15]. Briefly, prior to palmitate (C16:0) treatment, 100 mM palmitate solution was preheated to 60°C and was slowly dissolved in a 50°C preheated Bovine Serum Albumin (BSA, essentially fatty acid free) solution (15). The palmitate-BSA complex solutions were freshly diluted in DMEM without serum to a final concentration of 0.5 mmol/L palmitate/1% BSA. Cells were treated with palmitate-BSA complex solution after overnight serum deprivation. Palmitate-BSA complexes were incubated in heat block at 40°C for 30 min prior to cell exposure.

### Cell viability and genotoxicity

The cell viabilities of MNS-A or MNS-B were determined by trypan blue exclusion assay. Briefly, human hepatocytes were first seeded ( $2 \times 10^5$  cells/well) with plating medium (Invitrogen, Co.) in six-well tissue culture plates. The cells were incubated for 2 days and exposed to MNS-A or MNS-B at concentrations of 0, 10, 40 and 80 nM. The cells were resuspended in plating medium with trypan blue stain for 5 min and the trypan blue exclusion assay was performed as described previously [13]. The genotoxic effect of MNS-B was examined by GreenScreen HC assay without S9 metabolic activation (Cyprotex, Co., MA, USA). MNS-B was examined at the ranges of 0 to 640 nMs and the GFP fluorescence induction crossed the statistically defined significance threshold set at 1.5 (50%) at one or more test concentrations.

### Oil-red-O staining and triglyceride assay

To determine the triglyceride (TG) content and lipid accumulation, palmitate-treated hepatocytes were incubated with 20 nM MNS-A or B and measured by microscopy using an Oil-Red-O method [16]. Intracellular TG accumulation in each group was quantitatively analyzed using an L-Type TG M kit (Wako Chemicals Co., Japan) and normalized to the control with protein measurements using the BCA method.

### Protein extraction and western blot analysis

Human cell lines were lysed using RIPA lysis buffer and cell lysates were microcentrifuged at 12,000 g, 4°C for 10 minutes. Western blot analysis was performed as described previously [7]. Briefly, the sample proteins were electrophoretically separated using 4-12% NuPAGE® Novex® Bis-Tris Mini Gels and were transferred to a nitrocellulose membrane for 1 h at 40 V using a Western blot apparatus. The membrane was blocked for 2 h in 5% nonfat dry milk in TBST buffer at room temperature. The primary antibodies were incubated overnight at 4°C and then removed. The membrane was washed three times (5 min each) with TBST (Tris-buffered saline, 0.1% Tween 20). The membranes were then incubated with HRP-conjugated secondary antibody and were applied using the SuperSignal chemiluminescence kit. All immunoblots were scanned using a model Fluorchem M imaging system (Proteinsimple). Densitometry analysis for the expression of proteins was performed using ImageJ software. The protein levels were normalized with β-actin or total protein as appropriate.

### Animal studies

All mice (C57BL/6J, male) were purchased from the Jackson Laboratory (Bar Harbor, ME) and housed in a 12 hour light/dark cycle in a 21-24°C animal facility administered by the Division

of Animal Resources, Virginia Commonwealth University. All procedures were approved by the Institutional Animal Care and Use Committee of Virginia Commonwealth University (Protocol #: AD10001181). A total of 15 mice from 8 to 12 weeks of age were evaluated for 2 weeks following the administration of MNS-B in standard chow diet mice (CD, Harlan TD.7012). The drugs were administered once daily by oral gavage for a period of 2 weeks. The mice were monitored every day and their body weight were recorded on a weekly basis. At the endpoint, mice were fasted and sacrificed; blood and tissue samples were collected and biochemical analysis were performed.

### Statistical analysis and sample size estimation

Sample size estimations were performed using N Query Advisor 7.0. To test the hypothesis that change occurred incrementally from controls to NAFL to NASH with an effect size (mean levels controls vs. disease) of 1.25 for NAFL and 1.5 for NASH, and assuming a standard deviation of 25% for each of the groups and a power of 80% to detect changes at a p value of 0.05, a total of 6 subjects would be required in each arm. If the effect size was a 2-fold change in NASH and 1.5 fold change in NAFL, the sample size dropped to 3 subjects in each arm. Not knowing the exact standard deviation for each of the biologic parameters to be measured, a minimum sample size of 10-12 subjects for each group was planned. Western blot data for phosphorylated ratios were expressed as phosphorylated to total target protein while unphosphorylated proteins were normalized with  $\beta$ -actin. The RNA and protein levels for a given gene were compared across groups using Kruskal Wallis analysis of variance (ANOVA), a distribution-free test. A Dunn's post-test was used for multiple comparisons. Significance was set at a p value of 0.05 or 0.01.

## RESULTS

### AMPK $\alpha$ (Thr172) phosphorylation levels are decreased and increased ERK1/2 in NAFLD patients

A total of 10 subjects each with NASH or NAFL were compared to 8 lean and 10 obese controls with normal liver histology. The summary of demographic, clinical, and laboratory data were provided in our previous publication [15]. The data showed that the groups were well matched with respect to age, gender, and the racial distribution [15]. Subjects with NAFL or NASH had higher serum ALT (alanine aminotransferase) levels compared to obese and lean controls ( $p < 0.008$ ). Hepatic synthetic functions were normal across all the groups. There was a progressive decrease in mean hepatic AMPK $\alpha$  (Thr172) phosphorylation levels in NAFL and NASH patients compared to lean and obese control patients, whereas ERK1/2 phosphorylation levels were significantly increased (Figures 1A-1C,  $p < 0.01$ ). The mean levels of AMPK $\alpha$  phosphorylation were comparable in both control groups and were lower than those of NAFL or NASH patients. The AMPK $\alpha$  phosphorylation levels in NASH patients were somewhat lower than those with NAFL (Figures 1A and 1C,  $p < 0.05$ ). This result was accompanied by an increase in levels of ERK1/2 phosphorylation (Figures 1A and 1B,  $p < 0.01$ ).

### IL-6 levels were directly related to ERK1/2 phosphorylation and inversely related to AMPK $\alpha$ (Thr172) phosphorylation

In contrast to hepatic AMPK $\alpha$  phosphorylation levels, the levels of circulating IL-6, a liver-derived pro-inflammatory cytokine [15], increased progressively from lean normal to obese controls to

NAFL and then NASH (Figures 1C and 1D,  $p < 0.01$ ). The IL-6 levels in those with NAFL and NASH were significantly higher than the levels of either control group. Also, the levels in those with NASH were higher than in those with NAFL ( $p < 0.01$ ). The ERK1/2 phosphorylation levels were significantly higher in those with NAFL or NASH compared to the levels of either control group (Figure 1E,  $p < 0.01$ ). Circulating IL-6 levels were directly related to hepatic ERK1/2 phosphorylation and inversely related to hepatic AMPK $\alpha$  phosphorylation.

### MNS-A and B increase AMPK $\alpha$ (Thr172) phosphorylation and decrease ERK1/2 phosphorylation levels in PA or IL-6-treated hepatocytes

As expected, exposure to palmitate (0.5 mM) led to a significant decrease in AMPK $\alpha$  protein phosphorylation levels in human primary hepatocytes (HPH) and Huh-7 cells. In contrast, ERK1/2 phosphorylation levels were increased (Figures 2A and 2B,  $p < 0.01$ ). In order to determine if ERK1/2 inhibition leads to enhanced AMPK $\alpha$  activity, serum starved HPH and Huh-7 cells were incubated with two different ERK1/2 chemical inhibitors, 25  $\mu$ M U0126 for 20 min or 1  $\mu$ M PD18452 for 20 min [17]. Cells were then stimulated with 10 ng/ml IL-6 for 30 min. U0126 or PD18452 treatment of HPH and Huh-7 cells activated AMPK $\alpha$  and decreased ERK1/2 phosphorylation levels (Figures 2C and 2D,  $p < 0.01$ ). Moreover, incubation with 1 mM AICAR (AMPK activator) for 13 hours significantly increased AMPK $\alpha$  phosphorylation levels. ERK1/2 phosphorylation levels were increased in IL-6-treated hepatocytes (Figures 2E and 2F,  $p < 0.01$ ). Taken together, these data demonstrate that ERK1/2 inhibition allows AMPK $\alpha$  phosphorylation-dependent activation whereas AMPK $\alpha$  activation suppresses ERK1/2 phosphorylation levels in palmitate or IL-6-treated hepatocytes.

### MNS-A and MNS-B have no cells toxicity and genotoxicity in hepatocytes

Cells viability and genotoxicity are widely used by the pharmaceutical industry as the first step in screening assays for drugs [18,19]. We first examined the effect of MNS-A and MNS-B on cell viability in human hepatocytes using the trypan blue exclusion assay. The cell viability did not change by MNS-A and MNS-B in a dose-dependent manner with maximal dose of 80 nM for 24 h when compared to the cell viability of the controls (Supplementary Figure 1A). Next, a genotoxic assay was carried out with MNS-B by GreenScreen HC assay without S9 metabolic activation. MNS-B was negative in the range of 0 to 640 nMs for genotoxicity in the GreenScreen HC assay without metabolic activation. The GFP fluorescence induction crossed the statistically defined significance threshold set at 1.5 (50%) at one or more test concentrations (Supplementary Figure 1B). These data indicate that MNS-A and MNS-B have no detectable cytotoxicity by trypan blue exclusion assay in the 0-80 nM range and genotoxic effect by GreenScreen HC assay without S9 metabolic activation in the 0-640 nM range, respectively.

### MNS-A and MNS-B decrease lipid accumulation (lipid droplets) in hepatocytes

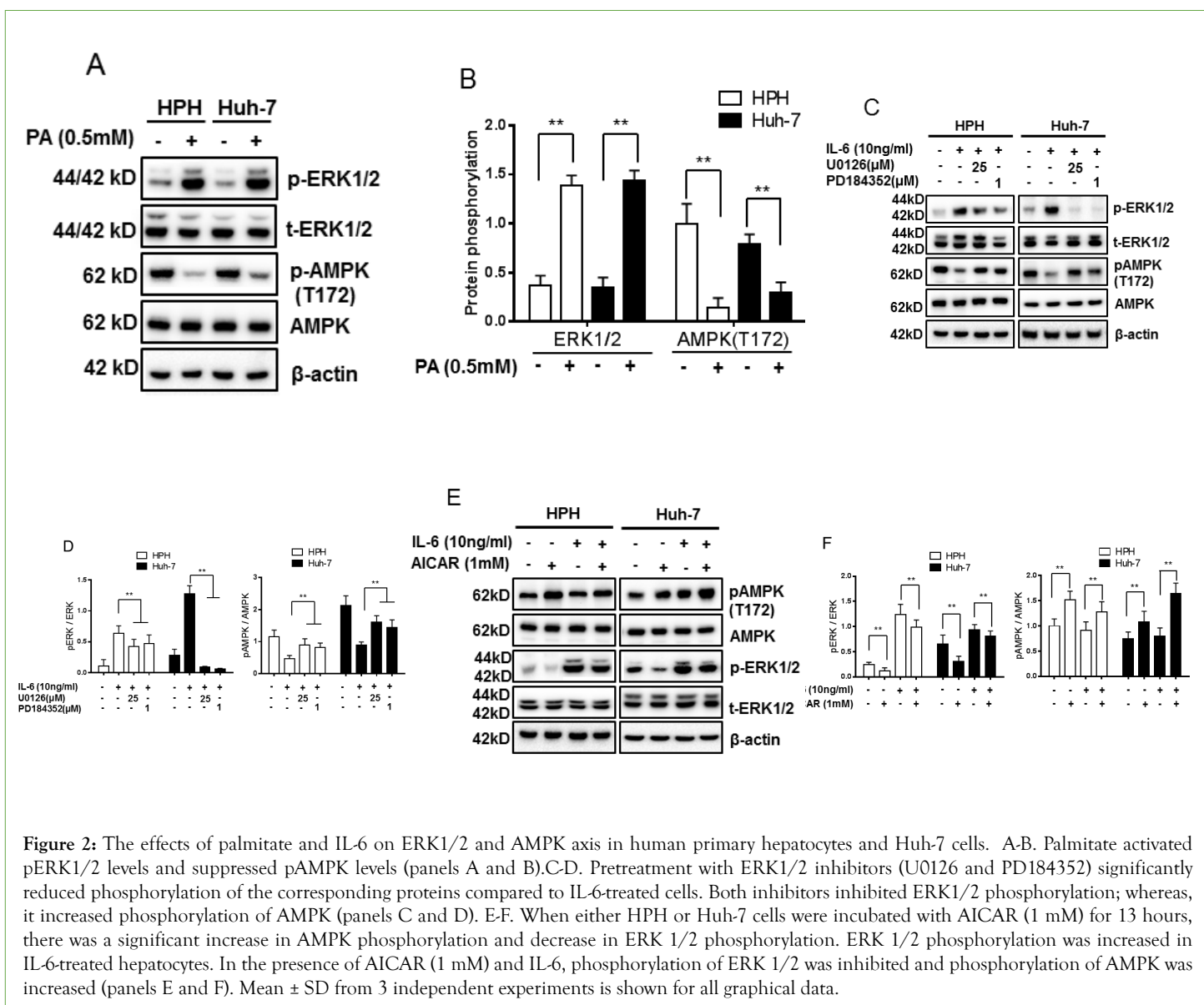
In order to examine hepatic lipid accumulation, Huh-7 cells were pre-incubated with MNS-A (20 nM) or MNS-B (20 nM) for 12 h and treated with palmitate (0.5 mM) for 8 h or 12 h. Hepatic lipid accumulation was observed in hepatocytes by Oil Red O staining. The quantitation of Triglycerides (TGs) levels was also determined using L-Type TG M kits (Wako chemicals Co.). The intracellular

lipid content and drops were significantly decreased in cells treated with MNS-A or MNS-B compared to control palmitate-treated hepatocytes (Figures 3A and 3B,  $p < 0.01$ ). 5'-AMP stimulates AMPK activation by activating upstream kinases, e.g. serine/threonine kinase 11 (LKB1) [20, 21],  $Ca^{2+}$ /calmodulin-dependent protein kinase  $\beta$  (CaMKK $\beta$ ) [20-22], and by inhibiting protein phosphatases (PP), e.g. PP2A, PP2C $\alpha$  and Ppm1E [23]. The current study shows that palmitate decreased cellular AMP: ATP ratio, which is conversely increased by MNS-A (20 nM) or MNS-B (20 nM) in palmitate-treated hepatocytes (Figure 3C,  $p < 0.01$ ). PP2A protein expression and activity were not affected by the presence of MNS-A and -B in palmitate-treated hepatocytes (Figures 3D and 3E). Next, to evaluate the effects of MNS-A and MNS-B on the hepatocyte AMPK pathway, Huh-7 cells were incubated with DMEM media in the presence and absence of palmitate. Both compounds increased palmitate-suppressed AMPK $\alpha$  activation, as assessed by the phosphorylation of AMPK $\alpha$  (Thr172) and its downstream target acetyl-CoA carboxylase (ACC) (Ser79), in hepatocytes (Figure 3F). Fatty acid synthase (FASN), ACC, and AMPK protein expression levels remained unchanged (Figure 3F). Taken together, these data indicate that MNS-A and MNS-B decrease palmitate-induced

lipid accumulation *via* an increase in the cellular AMP: ATP ratio, which increases AMPK $\alpha$  activation. MNS-A and MNS-B effects are independent of PP2A protein expression and activation in palmitate-treated hepatocytes.

### MNS-A and MNS-B inhibit ERK1/2 and induce AMPK $\alpha$ activation in palmitate or IL-6-treated hepatocytes

As shown in Figure 2, palmitate or IL-6 induced ERK1/2 phosphorylation and inhibited AMPK $\alpha$  phosphorylation in primary human hepatocytes. These data indicate that ERK1/2 counteracts AMPK $\alpha$  activation in palmitate or IL-6-treated hepatocytes. The specificity of the effects of MNS-A and MNS-B on the ERK1/2 and AMPK $\alpha$  phosphorylation levels were confirmed by the abrogation of the IL-6 or palmitate effects by ERK1/2 inhibitors, U0126, and PD18452 compared to control hepatocytes. As expected, palmitate or IL-6-induced phosphorylation of ERK1/2 was blunted by U0126 or PD18452, specific inhibitors of the ERK1/2 in hepatocytes. Also, MNS-A and MNS-B inhibited ERK1/2 and activated AMPK $\alpha$  phosphorylation (Figures 4A-4B,  $p < 0.01$  for both).



### Palmitate-induced autophagy was blocked by MNS-A and MNS-B in hepatocytes

Members of the PKC family, including PKC- $\theta$ , have been reported to be involved in autophagy induction by free fatty acids [23,24]. The current study shows that palmitate induced PKC- $\theta$  phosphorylation; whereas, MNS-A (20 nM) and MNS-B (20 nM) decreased PKC- $\theta$  phosphorylation in palmitate-treated hepatocytes (Figure 4C,  $p < 0.01$ ). Both p62 and LC3-II proteins are well known to play a role in autophagy by producing autophagosomes (APs) [25]. LC3, a protein known to be degraded exclusively by autophagy,

and p62 accumulates in the presence of saturated fatty acids or the combination of ammonium chloride/leupeptin [16]. To evaluate the effects of MNS-A and MNS-B on the autophagy, Huh-7 cells were incubated with palmitate or ammonium chloride/leupeptin. Both p62 and LC3-II expression levels were significantly decreased by MNS-A (20 nM) or MNS-B (20 nM) in palmitate-treated and ammonium chloride/leupeptin-treated hepatocytes (Figures 4D and 4E,  $p < 0.01$ ). These results indicate that MNS-A and MNS-B decrease the number and size of the APs and the content of AP substrates in palmitate-treated hepatocytes, decreasing its toxic effects.

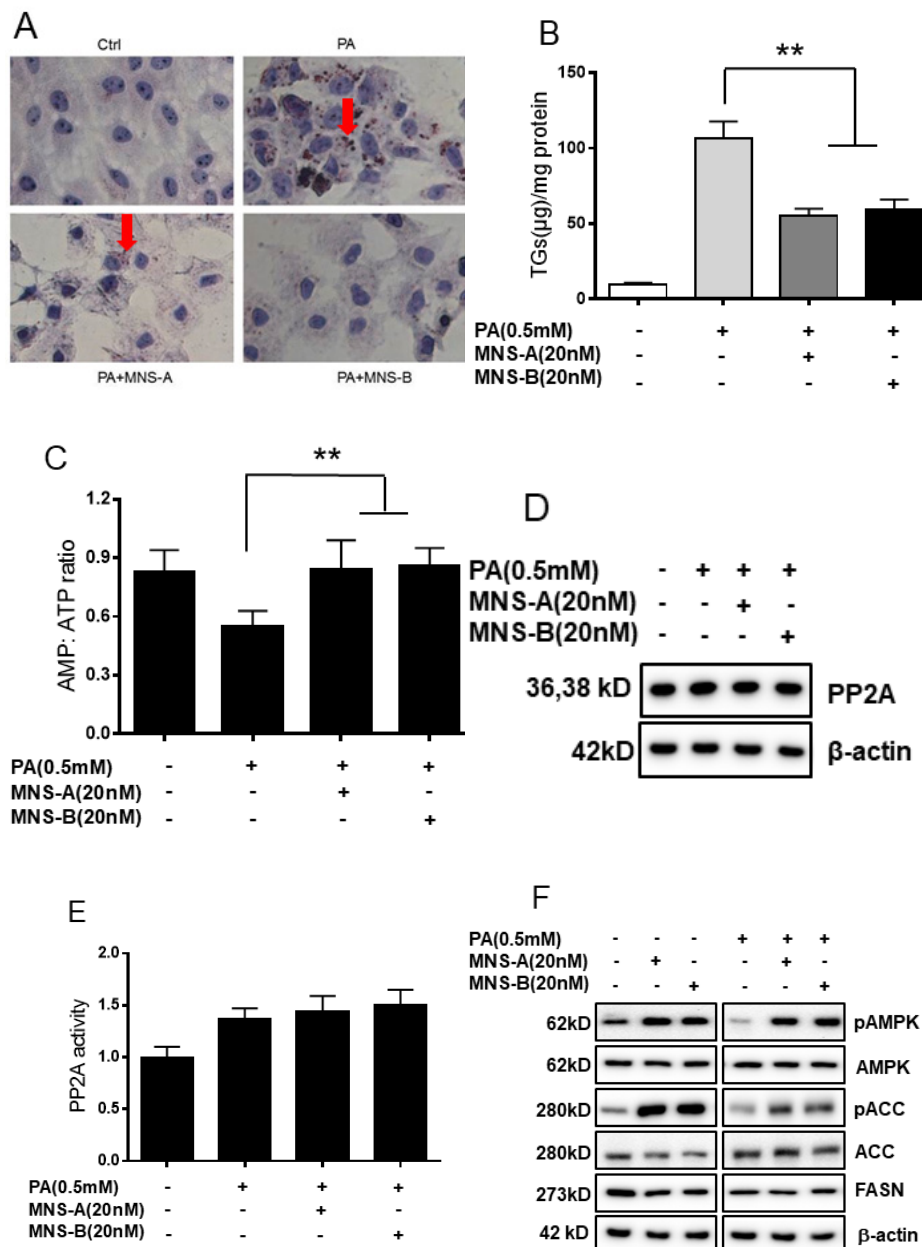


**Figure 3:** MNS-A and MNS-B decrease hepatic lipid accumulation through AMPK activation *via* an incensement of the AMP: ATP ratio. A-B. Huh-7 cells were pre-incubated with MNS-A (20 nM) or MNS-B (20 nM) for 12 h and treated with palmitate (0.5 mM) for 8 h or 12 h. Lipid accumulation and intracellular TGs were observed by Oil Red O staining and L-Type TG M kits, respectively. Both were significantly decreased in cells treated with MNS-A or MNS-B compared to control palmitate-treated hepatocytes. C-E. Palmitate decreased the cellular AMP: ATP ratio whereas the addition of MNS-A (20 nM) and MNS-B (20 nM) increased the cellular AMP: ATP ratio in palmitate-treated hepatocytes. PP2A expression and activity were not affected by palmitate, MNS-A, or MNS-B (panel D-E). F. Palmitate inhibited AMPK and ACC phosphorylation. MNS-A and MNS-B stimulated AMPK and ACC phosphorylation even in the presence of palmitate. Neither palmitate, MNS-A, or MNS-B affected FASN expression level. Mean  $\pm$  SD from 3 independent experiments is shown for all graphical data.

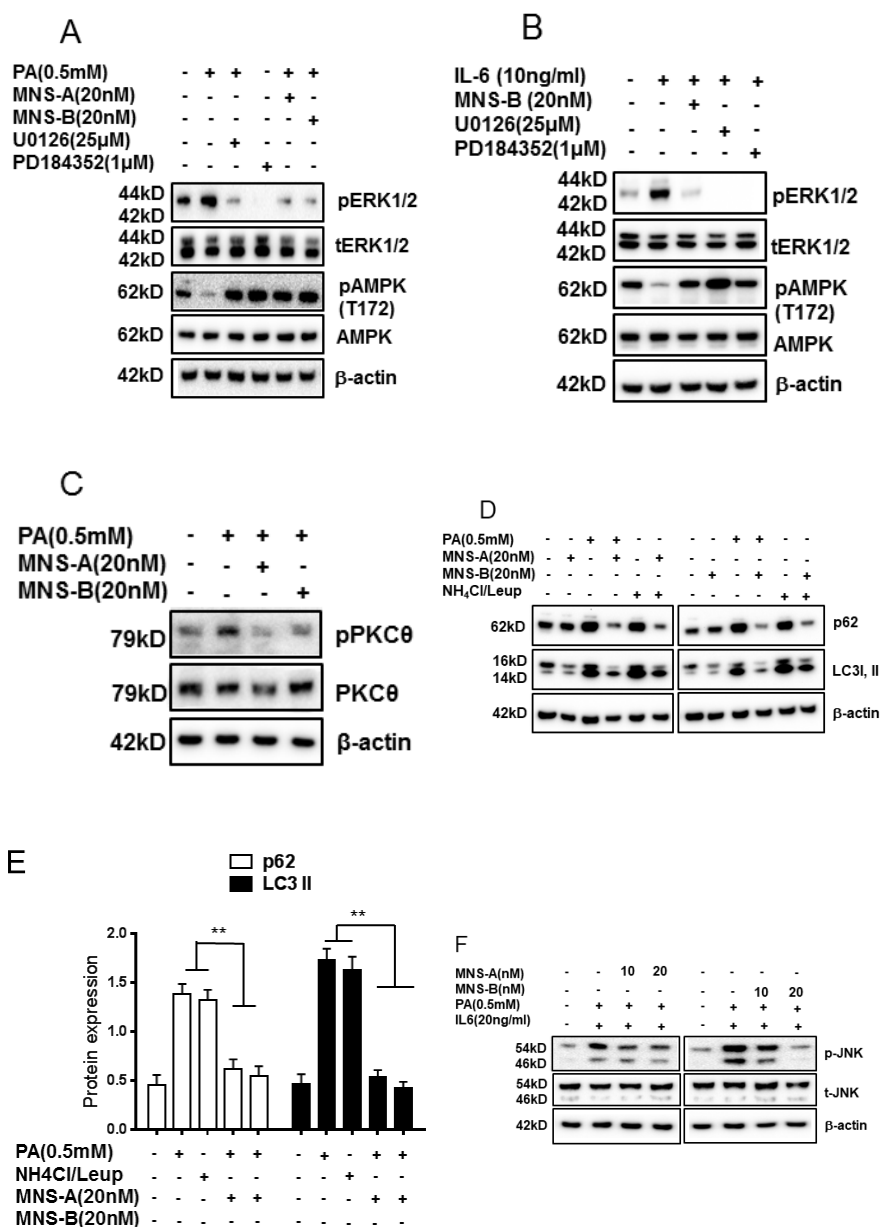


**Figure 4:** The effects of MNS-A and MNS-B on the ERK1/2: AMPK axis and autophagy in palmitate or IL-6 treated Huh-7 cells. A-B. Exposure to ERK inhibitors, U0126 and PD18452, showed similar effects as MNS-A or MNS-B. MNS-A and MNS-B suppressed ERK1/2 phosphorylation and increased AMPK phosphorylation in palmitate or IL-6-induced hepatocytes. C. Palmitate induced PKC- $\theta$  phosphorylation; whereas, MNS-A (20 nM) and MNS-B (20 nM) decreased PKC- $\theta$  phosphorylation in palmitate-treated hepatocytes. D-E. p62 and LC3-II protein levels were also significantly decreased by MNS-A (20 nM) or MNS-B (20 nM) in palmitate or ammonium chloride/leupeptin-treated human hepatocytes. These data indicate regulation of p62, LC3-II and PKC- $\theta$  phosphorylation levels by MNS-A and MNS-B in hepatocytes, which is attributed to a decrease in autophagy. Mean  $\pm$  SD from 3 independent experiments is shown for all graphical data.

### MNS-A and MNS-B regulate the gp130-STAT3 axis and inflammation in palmitate or IL-6-treated hepatocytes

The gp130-STAT3 axis plays key roles in ovarian cancer progression as well as in the pathogenesis of NAFLD [6-26]. To evaluate the gp130-STAT3 axis, human hepatocytes were treated with MNS-A or MNS-B in the presence of a normal glucose (5.5 mM) concentration with or without palmitate or IL-6. Palmitate or IL-6, activates Janus kinase (JAK)-signal transduction and transcription *via* the gp130/Stat3 axis [6]. In the current study, the expression of gp130 was markedly decreased by MNS-A (20 nM) or MNS-B (20 nM) in palmitate-treated hepatocytes. The Stat3 phosphorylation level was also markedly decreased in IL-6-treated hepatocytes (Figures

5A-5C,  $p < 0.01$  for gp130 or for pStat3). The specific effects of MNS-A and MNS-B on the gp130-STAT3 axis were confirmed by adding palmitate or IL-6 in hepatocytes. Furthermore, the JNK phosphorylation level was significantly increased in the palmitate and IL-6 treated hepatocytes (Figure 5D,  $p < 0.01$ ). Both MNS-A and -B were able to significantly inhibit the JNK phosphorylation level in the palmitate and IL-6 treated hepatocytes. An important observation to note is that MNS-B is dose dependent as shown by its increasing inhibitory effect at higher concentrations (Figure 5D,  $p < 0.01$ ). A schematic model was made that summarizes the *in vitro* effects of the MNS compounds in the etiology of NAFLD (Figure 5E).

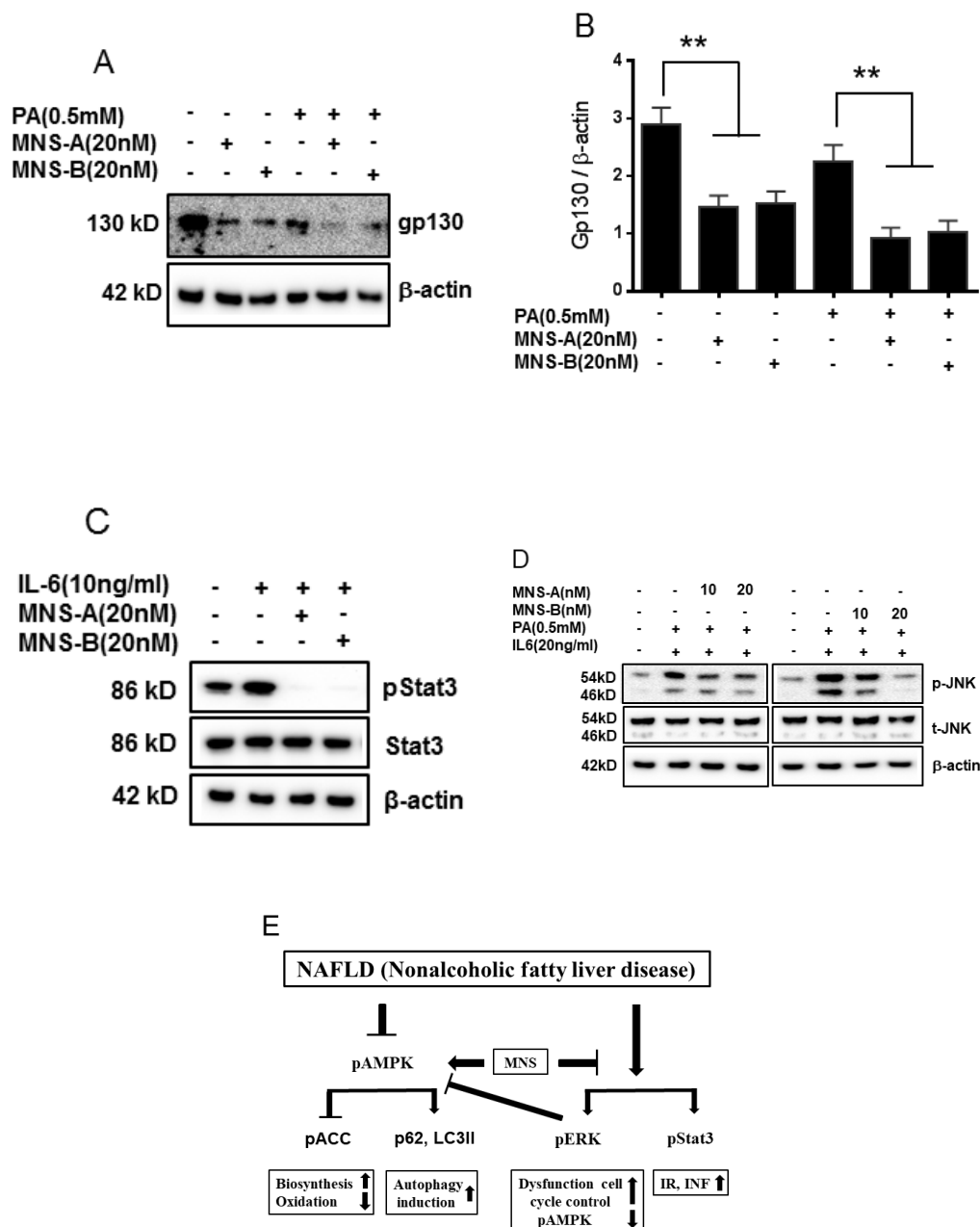


**Figure 5:** The effects of MNS-A and MNS-B on gp130-STAT3 axis and JNK activation in Huh-7 cells. A-C. Regulation of Gp130 protein and pSTAT3 levels by MNS-A and MNS-B in the presence and absence of palmitate in Huh-7 cells. D. Palmitate and IL-6 treatment increased the phosphorylation of JNK, a major protein involved in inflammatory signaling. MNS-A and MNS-B inhibited the JNK phosphorylation caused by the palmitate and IL-6 treatment. E. Schematic model of MNS (Manassantin) in the etiology of NAFLD. MNS stimulates AMPK activation and inhibits ERK1/2 phosphorylation, which decrease hepatic lipid accumulation and blocks palmitate-stimulated autophagy. These compounds also directly inhibits gp130 expression and Stat3 (T705) phosphorylation. Mean  $\pm$  SD from 3 independent experiments is shown for all graphical data.

### MNS-B regulates the phosphorylation levels of AMPK and ERK in normal diet-fed mice

Based on the results from the *in vitro* studies, an *in vivo* investigation was conducted to observe the effects of MNS-B on normal diet-fed mice. For this investigation, there were three sample groups: mice that were not treated with MNS-B (0 mg/kg) as a control and mice that were treated with 1 mg/kg or 5 mg/kg of MNS-B. All three groups were fed the normal diet. From the H & E staining images shown, there were no liver morphology and histology differences

observed among the three groups (Figure 6A). There were no significant differences observed in the end liver weights and changes in body weight, monitored for 2 weeks, among the three groups (Figures 6B and 6C). Among the observed parameters, the ALT level was shown to be decreased by the 5 mg/kg dosage of MNS-B (Table 1). Both dosages of MNS-B significantly decreased ERK1/2 phosphorylation levels and increased AMPK phosphorylation levels in the liver tissue (Figures 6D and 6E,  $p < 0.01$ ). Neither dosage of MNS-B had an effect on PARP and CASP3 expression levels (Figure 6D).

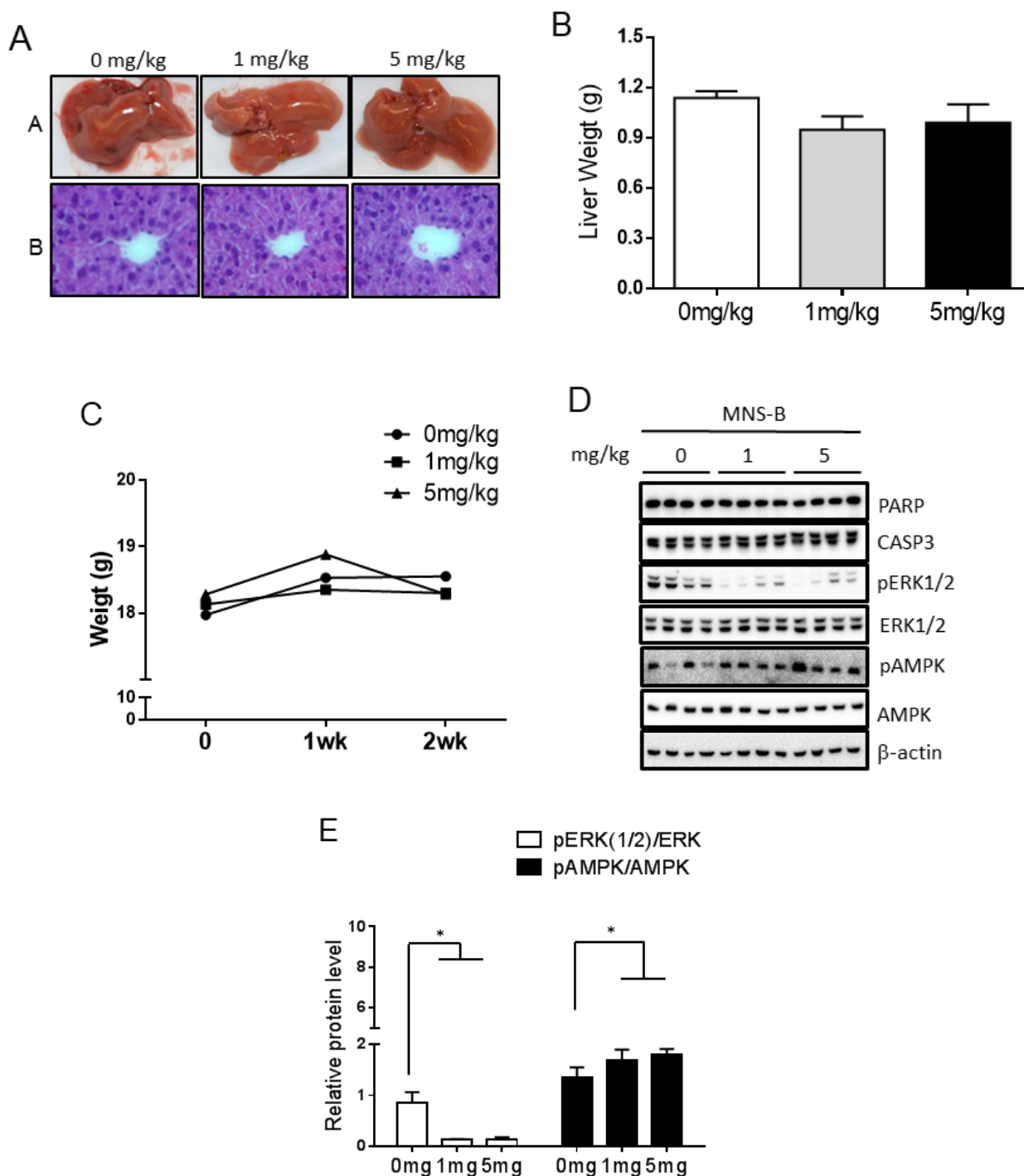


**Figure 6:** The effects of MNS-B on normal diet-fed mice. A. Liver morphology (upper A) and histology (H & E staining, upper B) in MNS-B-treated mice. There were no major differences regarding liver morphology and histology among three groups. B-C. Graphs depicting the end liver weight (B) and bodyweight changes (C) of the three groups. There was no statistical difference between the end liver weights and bodyweight changes between the control and treatment groups. D-E. The effect of MNS-B on protein expression levels in mice liver tissues using Western Blot. MNS-B did not significantly affect PARP and CASP-3 expression levels in a mice model. MNS-B significantly inhibited the phosphorylation of ERK1/2. MNS-B significantly increased the phosphorylation of AMPK and data is shown graphically in E. Means  $\pm$  SD from 3 independent experiments are shown for all graphical data. \* $P < 0.01$ .

## DISCUSSION

NAFLD is now the most common cause of chronic liver disease and the number of patients increase each year [1,16]. Patients with NAFLD also have an increased risk of cardiovascular diseases, heart attacks, and strokes [27]. Several studies have suggested that the ERK1/2-AMPK axis may regulate cancer cell death and Fc $\epsilon$ R1-dependent mast cell activation, its relationship to NAFLD are not

yet fully understood. We demonstrate that the hepatic ERK1/2-AMPK axis may be a key cellular mechanism regulating the pathogenesis of NAFLD under conditions of excess circulating IL-6 and/or free long chain fatty acids. The current study defines a key role for the differential regulation of ERK1/2 and AMPK in NAFL and NASH. In the liver samples of the NAFLD patient groups, there was a decrease in pAMPK $\alpha$  and an increase in pERK1/2

levels when compared to those of the lean and obese controls. ERK1/2-AMPK axis would thus be expected to contribute to the hepatic and systemic inflammatory state in subjects with NAFL or NASH. Given the overall decrease in hepatic AMPK $\alpha$  expression levels and increase in hepatic ERK1/2 activation in NAFLD as well as the reported increase in IL-6 in such cases, it is reasonable to postulate a role for IL-6 as a driver of NAFL and NASH. NAFLD is well known to be associated with lipotoxic stress such as palmitate, stearate [4,6], and pro-inflammatory cytokines including IL-6, TNF- $\alpha$ , and IL-8 [28,29]. Based on these observations, palmitate or IL-6 may be key players in the etiology of NAFLD.

Saururus Chinensis is a well-known oriental medicinal herb and has been reported to show biological activities in several cell types [9,13]. MNS-A and MNS-B inhibit the production of IL-1 $\beta$  and suppress ERK1/2 and p38 MAPK activation, but not JNK, in LPS-treated RAW 264.7 cells [13]. Other studies have reported that MNS has anti-inflammatory [13], anti-Human Immunodeficiency Virus (HIV) [30], hyperpigmentation disorder [31], and anti-plasmodial effects [14]. In the current study, we demonstrate that MNS-A and MNS-B counteract the effects of IL-6 and palmitate in inhibiting ERK1/2 activation but also activating AMPK $\alpha$  (Figures 3 and 4). These compounds showed no evidence of cellular or gene toxicities at concentrations well above those that showed benefit (Figure S1).

In summary, the current study demonstrates that MNS-A and MNS-B decreased hepatic lipid accumulation and attributed to a decrease in palmitate-induced autophagy *via* an ERK1/2-AMPK axis and PKC- $\theta$  modulation (Figures 4 and 5D). The gp130-Stat3 axis and hepatic inflammation by JNK phosphorylation were suppressed by MNS-A and MNS-B in IL-6 or palmitate-treated hepatocytes (Figure 5). A schematic model summarizing the effect of the MNS compounds on NAFLD etiology was made (Figure 5E). Observing the ameliorative *in vitro* effects of MNS-B, an *in vivo* investigation was performed using normal diet-fed mice to see if any physiological side effects occur and to elucidate the mechanism of the compound. There was no noticeable difference in liver weight, changes in body weight, and liver morphology and histology among the three groups (Figures 6A-6C). However, one point of interest is how MNS-B significantly decreased the ALT parameter level at a dosage of 5 mg/kg in the mice model (Table 1). Furthermore, MNS-B significantly upregulated the phosphorylation of AMPK (Figures 6D and 6E) which stimulates fatty acid oxidation and autophagy in order to combat against cellular energy deficiencies [32]. By increasing AMPK activation, MNS-B proves its potential in combating against disorders characterized by an excess amount of fat such as obesity and NAFLD. Additionally, MNS-B significantly inhibited ERK1/2 phosphorylation (Figures 6D and 6E) which plays a major role in many central signal transduction pathways [33]. By inhibiting ERK1/2 activation, MNS-B proves to be effective in maintaining a healthy liver condition without side effects in the mice model. In addition to these results, MNS-B did not appear to affect the expression levels of PARP and CASP3 proteins that signal apoptosis events (Figures 6D and 6E). Despite these positive results, the MNS compounds' effect in a NAFLD animal model remains unknown. However, based on our results that show MNS-B increases AMPK $\alpha$  and decreases ERK1/2 phosphorylation, we hypothesize that MNS-B can treat NAFLD by causing a switch to an energy-deficient state. This proposed mechanism is supported by a recent study by colleagues suggesting that MNS-B causes a bioenergy deficient state by inhibiting mitochondrial complex I in the mammalian model. As a result, the mammalian system

compensates for this deficient state by upregulating aerobic glycolysis through AMPK phosphorylation [34]. Further investigation is required to prove this mechanism of MNS-B's action and to see if the compound has a beneficial effect in a NAFLD animal model.

**Table 1:** Baseline laboratory data.

Parameter	0 mg/kg	1 mg/kg	5 mg/kg	P-value
	(n=5) Mean $\pm$ S.D.	(n=5) Mean $\pm$ S.D.	(n=5) Mean $\pm$ S.D.	
ALT (IU/l)	172.2 $\pm$ 37.4	116.0 $\pm$ 45.8	76.2 $\pm$ 17.7	<0.05*
AST (IU/l)	1090.7 $\pm$ 344.9	773.6 $\pm$ 282.6	782.0 $\pm$ 341.5	n.s*
Triglycerides (mg/dl)	65.6 $\pm$ 4.9	59.5 $\pm$ 4.9	68.0 $\pm$ 6.6	n.s*

Note: \*p<0.05 compared to mg/kg and 5 mg/kg groups.

## CONCLUSION

These data support the concept that MNS-A and MNS-B are considered to be potential therapeutic agents in treating NAFLD. Additional work will be required to confirm these concepts in an appropriate animal model. If successful, this could lead to clinical studies for treating NAFLD and possibly NASH.

## ACKNOWLEDGEMENTS

### Grant support

1. The work was supported by the following grants from the NIH to Dr. Sanyal-RO1 DK 105961 and T32 DK 007150.
2. This work was carried out with the support of "Cooperative Research Program for Agriculture Science & Technology Development (Project No. PJ90693833)" Rural Development Administration, Republic of Korea to Dr. Min.
3. The work was supported by the grants from the VCU's CTSA and the CCTR Endowment Fund of Virginia Commonwealth University to Dr. Min.

## REFERENCES

1. Browning JD, Szczepaniak LS, Dobbins R, Nuremberg P, Horton JD, Cohen JC, et al. Prevalence of hepatic steatosis in an urban population in the United States: impact of ethnicity. *Hepatology*. 2004;40(6):1387-1395.
2. Younossi ZM, Koenig AB, Abdelatif D, Fazel Y, Henry L, Wymer M. Global epidemiology of nonalcoholic fatty liver disease-meta-analytic assessment of prevalence, incidence, and outcomes. *Hepatology*. 2016;64(1):73-84.
3. Sanyal AJ, Campbell-Sargent C, Mirshahi F, Rizzo WB, Contos MJ, Sterling RK, et al. Nonalcoholic steatohepatitis: association of insulin resistance and mitochondrial abnormalities. *Gastroenterology*. 2001;120(5):1183-1192.
4. Chitturi S, Abeygunasekera S, Farrell GC, Holmes-Walker J, Hui JM, Fung C, et al. NASH and insulin resistance: insulin hypersecretion and specific association with the insulin resistance syndrome. *Hepatology*. 2002;35(2):373-379.
5. Ekstedt M, Franzén LE, Mathiesen UL, Thorelius L, Holmqvist M, Bodemar G, et al. Long-term follow-up of patients with NAFLD and elevated liver enzymes. *Hepatology*. 2006;44(4):865-873.
6. Min HK, Mirshahi F, Verdianelli A, Pacana T, Patel V, Park CG, et al. Activation of the GP130-STAT3 axis and its potential implications in nonalcoholic fatty liver disease. *Am J Physiol Gastrointest Liver Physiol*. 2015;308(9):G794-803.

7. Min HK, Kapoor A, Fuchs M, Mirshahi F, Zhou H, Maher J, et al. Increased hepatic synthesis and dysregulation of cholesterol metabolism is associated with the severity of nonalcoholic fatty liver disease. *Cell Metab.* 2012;15(5):665-674.
8. Joshi-Barve S, Barve SS, Amancherla K, Gobejshvili L, Hill D, Cave M, et al. Palmitic acid induces production of proinflammatory cytokine interleukin-8 from hepatocytes. *Hepatology.* 2007;46(3):823-830.
9. Oliveira CP, Sanches PD, de Abreu-Silva EO, Marcadenti A. Nutrition and Physical Activity in Nonalcoholic Fatty Liver Disease. *J Diabetes Res.* 2016.
10. Smith BW, Adams LA. Nonalcoholic fatty liver disease and diabetes mellitus: pathogenesis and treatment. *Nat Rev Endocrinol.* 2011;7(8):456-465.
11. Mazza A, Fruci B, Garinis GA, Gituliano S, Malaguarnera R, Belfiore A. The role of metformin in the management of NAFLD. *Exp Diabetes Re.* 2012.
12. Sanyal AJ, Uenalp A. Pioglitazone, vitamin E, or placebo for nonalcoholic steatohepatitis reply. *N Engl J Med.* 2010;363(12):1186.
13. Park HC, Bae HB, Jeong CW, Lee SH, Jeung HJ, Kwak SH. Effect of manassantin B, a lignan isolated from *Saururus chinensis*, on lipopolysaccharide-induced interleukin-1 $\beta$  in RAW 264.7 cells. *Korean J Anesthesiol.* 2012;62(2):161.
14. Kraft C, Jenett-Siems K, Köhler I, Tofern-Reblin B, Siems K, Bienzle U, et al. Antiplasmodial activity of sesquignans and sesqueneolignans from *Bonamia spectabilis*. *Phytochemistry.* 2002;60(2):167-173.
15. Min HK, Maruyama H, Jang BK, Shimada M, Mirshahi F, Ren S, et al. Suppression of IGF binding protein-3 by palmitate promotes hepatic inflammatory responses. *FASEB J.* 2016;30(12):4071-4082.
16. Singh R, Kaushik S, Wang YJ, Xiang YQ, Novak I, Komatsu M, et al. Autophagy regulates lipid metabolism. *Nature.* 2009;458(7242):1131-U64.
17. Dokladda K, Green KA, Pan DA, Hardie DG. PD98059 and U0126 activate AMP-activated protein kinase by increasing the cellular AMP: ATP ratio and not *via* inhibition of the MAP kinase pathway. *FEBS Lett.* 2005 3; 579(1):236-240.
18. Hansen J, Bross P. A cellular viability assay to monitor drug toxicity. *Methods Mol Biol.* 2010;648:303-311.
19. Witte I, Plappert U, de Wall H, Hartmann A. Genetic toxicity assessment: Employing the best science for human safety evaluation, part III: The comet assay as an alternative to *in vitro* clastogenicity tests for early drug candidate selection. *Toxicol Sci.* 2007;97(1):21-26.
20. Shackelford DB, Shaw RJ. The LKB1-AMPK pathway: metabolism and growth control in tumour suppression. *Nat Rev Cancer.* 2009;9(8):563-575.
21. Sun L, Liu X, Fu H, Zhou W, Zhong D. 2-Deoxyglucose suppresses ERK phosphorylation in LKB1 and Ras wild-type non-small cell lung cancer cells. *PloS one.* 2016;2911(12):e0168793.
22. Fujiwara Y, Kawaguchi Y, Fujimoto T, Kanayama N, Magari M, Tokumitsu H. Differential AMP-activated Protein Kinase (AMPK) Recognition Mechanism of Ca<sup>2+</sup>/Calmodulin-dependent Protein Kinase Kinase Isoforms. *J Biol Chem.* 2016;291(26):13802-13808.
23. Salminen A, Kaarniranta K. AMP-activated protein kinase (AMPK) controls the aging process *via* an integrated signaling network. *Ageing Res Rev.* 2012;11(2):230-241.
24. Sakaki K, Wu J, Kaufman RJ. Protein kinase C $\theta$  is required for autophagy in response to stress in the endoplasmic reticulum. *J Biol Chem.* 2008;283(22):15370-15380.
25. Eskelinen EL, Saftig P. Autophagy: a lysosomal degradation pathway with a central role in health and disease. *Biochim Biophys Act.* 2009;1793(4):664-673.
26. Yu H, Lee H, Herrmann A, Buettner R, Jove R. Revisiting STAT3 signalling in cancer: new and unexpected biological functions. *Nat Rev Cancer.* 2014;14(11):736-746.
27. Anstee QM, Targher G, Day CP. Progression of NAFLD to diabetes mellitus, cardiovascular disease or cirrhosis. *Nat Rev Gastroenterol Hepatol.* 2013;10(6):330-44.
28. Cusi K. Role of Obesity and Lipotoxicity in the Development of Nonalcoholic Steatohepatitis: Pathophysiology and Clinical Implications. *Gastroenterology.* 2012;142(4):711-U109.
29. Feldstein AE, Werneburg NW, Canbay A, Guicciardi ME, Bronk SF, Rydzewski R, et al. Free fatty acids promote hepatic lipotoxicity by stimulating TNF- $\alpha$  expression *via* a lysosomal pathway. *Hepatology.* 2004;40:185-194.
30. Wang M, Tao L, Xu H. Chinese herbal medicines as a source of molecules with anti-enterovirus 71 activity. *Chin Med.* 2016;11(1):1-26.
31. Seo CS, Lee WH, Chung HW, Chang EJ, Lee SH, Jahng Y, et al. Manassantin A and B from *Saururus chinensis* inhibiting cellular melanin production. *Phytother Res.* 2009;23(11):1531-6.
32. Foretz M, Even PC, Viollet B. AMPK activation reduces hepatic lipid content by increasing fat oxidation *in vivo*. *Int J Mol Sci.* 2018;19(9):2826.
33. Guégan JP, Frémin C, Baffet G. The MAPK MEK1/2-ERK1/2 pathway and its implication in hepatocyte cell cycle control. *Int J Hepatol.* 2012.
34. Ma Y, Min HK, Oh U, Hawkrigde AM, Wang W, Mohsin AA, et al. The lignan manassantin is a potent and specific inhibitor of mitochondrial complex I and bioenergetic activity in mammals. *J Biol Chem.* 2017;292(51):20989-20997.